Bioconjugate Chemistry

Article

Beyond gene transfection with methacrylate-based polyplexes – the influence of the amino substitution pattern

Ulrich S. Schubert, Tanja Bus, Martin Reifarth, Johannes C. Brendel, Stephanie Hoeppener, Anja Traeger, and Anne-Kristin Trützschler

Bioconjugate Chem., **Just Accepted Manuscript** • DOI: 10.1021/acs.bioconjchem.8b00074 • Publication Date (Web): 01 May 2018

ACS Publications

is published by the American Chemical Society. 1155 Sixteenth Street N.W., Washington, DC 20036

Beyond Gene Transfection with Methacrylate-based Polyplexes – The Influence of the Amino Substitution Pattern

Anne-Kristin Trützschler,[‡,§,†] Tanja Bus,[‡,§,†] Martin Reifarth,[‡,§,#,$] Johannes C. Brendel,[‡,§] Stephanie Hoeppener,[‡,§] Anja Traeger,[‡,§,] Ulrich S. Schubert,[‡,§,]**

[‡] Laboratory of Organic and Macromolecular Chemistry (IOMC), Friedrich Schiller University Jena, Humboldtstrasse 10, 07743 Jena, Germany

[§] Jena Center for Soft Matter (JCSM), Friedrich Schiller University Jena, Philosophenweg 7, 07743 Jena, Germany

[#] Institute of Physical Chemistry and Abbe Center of Photonics, Friedrich Schiller University Jena, Helmholtzweg 4, 07743 Jena, Germany

[$] Leibniz Institute of Photonic Technology, Albert-Einstein-Strasse 9, 07745 Jena, Germany

† The authors contributed equally to this work

Email: ulrich.schubert@uni-jena.de, anja.traeger@uni-jena.de

ABSTRACT

Methacrylate-based polymers represent promising non-viral gene delivery vectors, since they offer a large variety of polymer architectures and functionalities, which are beneficial for specific demands in gene delivery. In combination with controlled radical polymerization techniques, such as the reversible addition-fragmentation chain transfer polymerization, the synthesis of well-defined polymers is possible. In this study we prepared a library of defined linear polymers based on (2-aminoethyl)-methacrylate (AEMA), *N*-methyl-(2-aminoethyl)-methacrylate (MAEMA) and *N,N*-dimethyl-(2-aminoethyl)-methacrylate (DMAEMA) monomers, bearing pendant primary, secondary and tertiary amino groups, and investigated the influence of the substitution pattern on their gene delivery ability. The polymers and the corresponding plasmid DNA complexes were investigated regarding their physicochemical characteristics, cytocompatibility and transfection performances. The non-viral transfection by methacrylate-based polyplexes differs significantly from poly(ethylene imine)-based polyplexes, as a successful transfection is not affected by the buffer capacity. We observed that polyplexes containing a high content of primary amino groups (AEMA) offered the highest transfection efficiency, whereas polyplexes bearing tertiary amino groups (DMAEMA) exhibited the lowest transfection efficiency. Further insights into the uptake and release mechanisms could be identified by fluorescence and transmission electron microscopy, emphasizing the theory of membrane-pore formation for the time-efficient endosomal release of methacrylate-based vectors.

INTRODUCTION

In the last century the intensive research on major human diseases has shown that a wide variety of diseases originate from dysfunction in protein expression. With the increasing knowledge about gene regulation and the role of RNA, personalized therapies on the basis of nucleic acids became feasible. Due to the instability of naked nucleic acids against nucleases and the limited direct cellular uptake,[1] the use of delivery systems, called vectors, is essential for efficient therapeutic approaches. Besides viral vectors, synthetic systems gain increasing attention in the field of gene delivery. Despite the high transfection efficiency of viral gene delivery vectors,[2] the potential immune response on the natural viral proteins, the limitations in the size of the DNA and the difficulties in the scale-up of these systems make non-viral systems more favorable.[3] In accordance, the structures and efficiencies of polymeric delivery systems have constantly been improved, since the first polycation-mediated transfection in 1965[4] and the first polymer-targeted gene delivery in the late 1980s have been introduced.[5, 6] Different bottlenecks during the transfection processes have been described so far.[7] Thereby, a high molar mass, the presence of cationic charges as well as a buffering capacity at low pH values were discussed to be beneficial for (i) the formation of the polymer/nucleic acid complex, (ii) the attachment of this complex to cellular membranes and the associated uptake by endocytosis, (iii) as well as the endosomal escape and dissociation of the cargo from the polymer. To date linear poly(ethylene imine) (lPEI) represents the most frequently applied and efficient polymer for gene delivery. The secondary amino groups along the backbone are partially protonated at physiological conditions, which enable the binding of nucleic acids and the buffering of acidifying endosomes as postulated by the popular "proton sponge" hypothesis.[8, 9] This theory describes a potential escape strategy from endo-lysosomes by the increase of the charge density due to further protonation leading to an enhanced influx of chloride ions and water. Consequently, the increasing osmotic pressure causes the rupture of the endosomal membrane and hence, the release of the vector within the cytsoplasm. Besides lPEI, which comprises mainly secondary amino groups, other materials and amino functionalities have been studied regarding their transfection performance including polymers like poly-L-lysine (PLL, primary amino groups), poly(*N,N*-dimethyl(aminoethyl) methacrylate)

(PDMAEMA, tertiary amino groups) and branched PEI (bPEI, primary, secondary and tertiary amino groups). To gain deeper insights into the impact of the different amino functionalities it is important to investigate the transfection performance with defined structures. As a consequence, the reversible addition-fragmentation chain transfer polymerization technique (RAFT), which tolerates a wide range of functional groups and enables the controlled synthesis of well-defined structures, represents a promising tool in polymer-based gene delivery.[10, 11] In particular, the structural versatility of methacrylate-based polymers allows the introduction of all mentioned different amino moieties into a similar polymer structure and, thus, a direct comparison of the impact of primary, secondary and tertiary amino groups. So far, only a few studies investigated the influence of this degree of substitution on the final transfection efficiency. Primary, secondary as well as tertiary amino groups were studied separately on polymer structure and functionality use by groups like Reineke and coworkers as well as by Zhu *et al.*.[12-14] Palermo *et al.* revealed that primary and tertiary amino groups in methacrylate-based copolymers complex the phosphate head groups of an artificial lipid bilayer, showing higher membrane internalization of the primary amino groups.[15] This theory is supported by earlier findings of disruptive peptides, which evolve into the membrane to create pathways for other molecules to escape into the cytosol.[16-18] Nevertheless, a thorough comparison of structurally similar polymers comprising primary, secondary and tertiary amino groups is still missing. Up to our knowledge, previous reports included either additional functional domains or monomers, or lack at least one of the structural amino varieties.

Within this study we focused on the controlled RAFT synthesis of 2-(*N,N*-dimethylamino)ethyl methacrylate, *N*-methyl-*N*-*tert*-butyloxycarbonyl-(2-aminoethyl)-methacrylate (BocMAEMA) and *N*-*tert*-butyloxycarbonyl-(2-aminoethyl)-methacrylate (BocAEMA) to create a library of linear statistical homo- and copolymers with varying amino functionalities. Based on this library, we were able to investigate the influence of different compositions of primary, secondary and tertiary amino groups in linear polymers on the transfection performance and to elucidate an optimal polymer composition. The polymers were characterized concerning their polyplex formation, cytocompatibility, their extra- and intracellular fate focusing on uptake and endosomal release.

RESULTS AND DISCUSSION

Polymer preparation and characterization

To systematically investigate the influence of secondary amino groups in combination with primary and tertiary amino groups on the transfection efficiency, a library of linear statistical polymers was synthesized *via* RAFT polymerization.[10, 19] The direct polymerization of AEMA with MAEMA and/or DMAEMA led to hydrogels during the polymerization process. This side reaction is probably caused by the basic effect of the amino groups containing methacrylate monomers, which resulted in the aminolysis of the esters or the RAFT group. The cycling or branching reaction induced by the aminolysis of the methacrylate ester unit was previously described and is commonly used for crosslinking of polymers.[20] Another possible reason for the gel formation might be the aminolysis of the RAFT end group causing intermolecular disulfide bridges.[21-23] Therefore, BocAEMA and BocMAEMA were synthesized starting with the Boc-protection of the corresponding ethanolamine according to literature reports.[24-27]

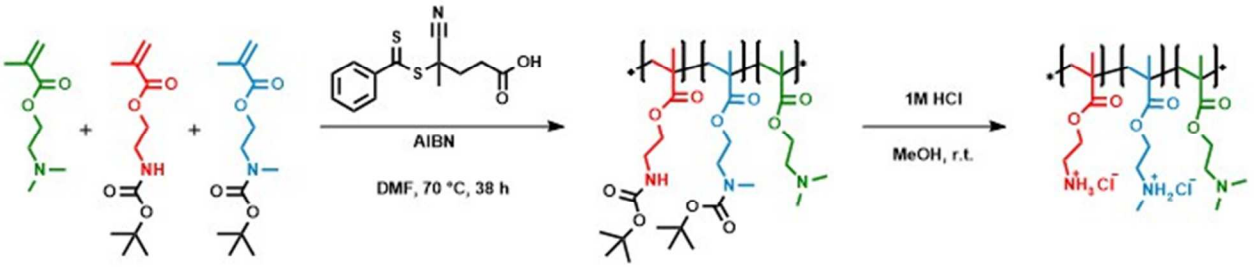

Scheme 1. Schematic representation of the RAFT-polymerization and deprotection reaction of the terpolymer containing Boc-protected primary (red), secondary (blue) and tertiary (green) amino groups containing monomers.

Due to the Boc–protection of the primary and secondary amino groups during the synthesis the hydrogel formation can be avoided during the polymerization process. The polymerization was performed in DMF at 70 °C for 40 h with a M/CTA feed of 240, with a CTA/I ratio of 4 and monomer ratios of the copolymers or terpolymers of 50:50 or 1/3, respectively (Scheme 1). The kinetics of the co- and terpolymerization revealed a controlled polymerization with narrow dispersity and a statistical distribution of the monomers (see SI Figure S1 and S2). For the copolymerization of BocAEMA and DMAEMA similar reactivity rations were already described by Zhu *et al.*[12] The aim for the final molar mass of the

synthesized polymers was at least 20 kDa, which represents a compromise considering the enhancement of the transfection efficiency *versus* an increasing toxicity with increasing molar mass and the opportunity for controlled polymer synthesis.[28, 29]

An overview of the synthesized Boc-protected polymer library (**PBM** to **PBMA**) is provided in Table 1. In the following, the polymers are named using "P" for polymer, "B" for the presence of Boc-protected AEMA and/or MAEMA units and the combination of letters "D", "M" and "A" for the presence of primary (A), secondary (M) or tertiary amino group containing monomers (D), respectively. All polymers featured molar masses in the range of 33 to 54 kDa and narrow distributions (see Figure 1A). In the ^{1}H-NMR spectra of the homo- and copolymers characteristic methylene signals of the protection group can be seen at 1.43 ppm (see SI Figure S3). The resulting compositions were calculated from ^{1}H-NMR using the ratio of the specific signals of the secondary (δ 2.93 ppm) and tertiary amine (δ 2.25 ppm) containing units, which are assigned to the methyl groups at the amino function. The ratio of those methyl signals to the methylene signal (δ 4.02 ppm) of all units neighboring the ester function in the backbone provides the mole fraction of each monomer.

Table 1. Selected characterization data of the Boc-protected polymers.

Polymer	M_n[a] [g mol^{-1}]	$Đ$	*n [mol%]*[b] DMAEMA	*n [mol%]*[b] BocMAEMA	*n [mol%]*[b] BocAEMA
PBM	35,600	1.08	-	100	-
PBA	33,800	1.10	-	-	100
PBDM	34,400	1.16	60	40	-
PBDA	49,800	1.19	57	-	43
PBMA	54,600	1.14	-	50	50
PBDMA	46,200	1.25	33	33	33

[a]Molar mass and dispersity were determined by size exclusion chromatography (DmAc, 0.21% LiCl, PMMA calibration). [b] The molar percentage was determined by ^{1}H-NMR.

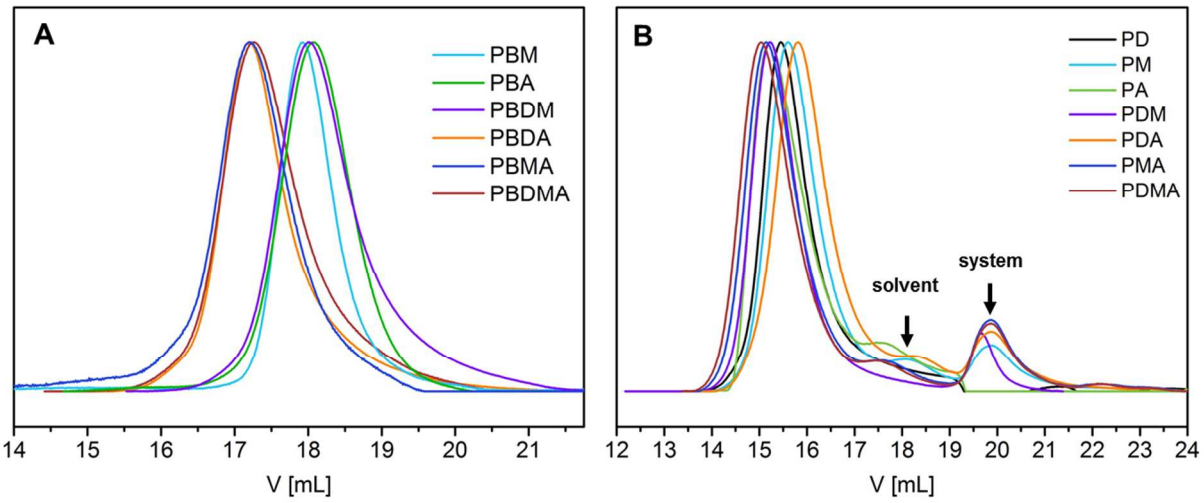

Figure 1. (A) Size exclusion chromatography curves (DmAc, 0.21% LiCl, PMMA calibration) of the Boc-protected polymer library showing narrow dispersities. **(B)** SEC curves (water, 0.1% trifluoroacetic acid, 0.1 M NaCl, system peak @ 20 mL) of deprotected polymer library showing monomodal distributions.

As no Boc-protection is required, the polymerization of the PDMAEMA homopolymer (**PD**) was directly performed in ethanol using 4,4′-azobis(4-cyanopentanoic acid) as initiator at 70 °C for 20 h. The other Boc-protected polymers of the library (**PBM** to **PBDMA**) were finally deprotected using 1 M hydrochloric acid in methanol. A complete deprotection of the polymers was confirmed by HSQC-NMR at a polymer concentration of 200 mg mL^{-1}, which did not show any residual ^{1}H-signal in the typical range at 1.44 ppm for the methyl groups of the Boc-protection group and no corresponding ^{13}C signal (see SI Figure S4). The results of the characterization experiments are summarized in Table 2. The characterization of the water-soluble deprotected library was performed by size exclusion chromatography on an AppliChrom ABOA CatPhil system, which revealed only small interactions with the cationic polymers (Figure 1B). The determination of the molar masses was conducted by asymmetric flow field-flow fractionation (AF4) coupled with multi-angle laser light scattering (MALLS) detection showing narrow distributions and molar masses in the range of 21 to 37 kDa. With regard to the missing appropriate size exclusion standards (dextrane used for aqueous SEC) for cationic methacrylate systems the determination of the molar masses and the dispersities is more accurate by utilizing the MALLS

detection.[30] However, the AF4 measurement will always tend to underestimate the values for dispersitiy in comparison with other MALLS coupled techniques due to the architecture of the AF4 channel including a membrane with a cutoff of 10 kDa.[31]

Table 2. Selected characterization data of the co- and homopolymers.

Polymer	M_{nAF4}[a]	$Đ_{AF4}$[a]	Mn_{SEC}[b]	$Đ_{SEC}$[b]	DP[d]	pK_a
PD	26,200	1.09	29,000[c]	1.09[c]	185	7.45
PM	24,000	1.21	13,400	2.04	167	8.40
PA	21,400	1.10	11,700	1.98	163	8.19
PDM	31,500	1.14	17,900	2.15	208	7.97
PDA	37,000	1.12	16,500	2.19	249	7.83
PMA	46,000	1.28	20,000	2.26	348	8.29
PDMA	36,000	1.27	21,800	2.35	250	8.03

[a]Molar masses and dispersities were determined by AF4 using the MALLS detector. [b and c] Molar mass was determined by size exclusion chromatography ([b] 0.1 % TFA, 0.1M NaCl, dextran calibration/[c] DmAc, 0.21% LiCl, PMMA calibration). [d] The degree of polymerization was calculated from AF4 results and ^{1}H-NMR determining the ratio of monomers. pK_a value was calculated from the titration curves (see SI Figure S5).

In additional titration experiments, the pK_a values of the homo- and copolymers **PD** to **PDMA** were determined to be in the range from pH 7.45 to 8.40 (Table 2). The later used physiological ionic strength was mimicked by the addition of 150 mM NaCl. In Figure S5, the titration curves are shown starting at around pH 2 and plotted against the volume of 0.1 M NaOH solution added to the polymer solution of 10 mg mL^{-1}. The calulation of the pK_a value was performed by fitting the obtained curves with a FTT fit after smoothing the plot to avoid artefacts. The turning points were determined by the differentiation of the fitted curves and the pK_a value was calculated by the Henderson-Hasselbalch equation (2) (see experimental section). For PDMAEMA the pK_a was previously described to be 7.5 by van de Wetering *et al.*, which is in accordance with our result for the **PD** polymer (pK_a = 7.45).[32] These results confirm that at

typical cell culture conditions at a pH value of 7.2 to 7.4, at least half of the amino functions of the polymers are in a protonated state and can, therefore, bind and condense negatively charged nucleic acids, thus forming polyplexes.

The calculation of the buffer capacity was performed for qualitative comparison from the titration data according to equation (1) and was plotted as a function of the pH value (Figure S6). For the calculation of β, d(pH) was set to 1 as it is defined from IUPAC. D(OH^-) was calculated from the volume of sodium hydroxide solution used for the change of 1 pH unit.[33]

$$\beta = \frac{d\, n(OH^-)}{d\, pH} \qquad (1)$$

Tested polymers revealed buffer capacities in the range of pH 6.0 to 10.0. Homo- or copolymers with a high content of primary and secondary amino groups (**PM**, **PA**, **PMA** and **PDMA**) exhibited good buffer capacities at more basic conditions of pH 8.0 and above, while polymers with increasing content of tertiary amino groups (**PD**, **PDM**, **PDA**) tend to show also buffer capacities from neutral to acidic conditions in agreement with the increase in DMAEMA content. In particular, for **PD**, increased buffer capacities over the whole range from pH 6 to pH 8 could be observed. With regard to the "proton sponge" theory, it can be assumed that the sample **PD** most probably possesses the highest potential of enhancing endosomal release. Therefore, we examined the transfection potential of the methacrylate-based polymer library with a particular focus on the influence of different amino functionalities in the following studies, which includes cytocompatibility, cellular uptake and polymer-mediated escape.

Cytocompatibility

The success of newly designed synthetic transfection vectors crucially depends on their interaction with cellular membranes, the first biological barrier along the intracellular uptake process, which correlates with the overall cell viability. To investigate the cytotoxic potential of the methacrylate-based homo- and copolymers *in vitro*, we performed a resazurin-based cell viability assay with L929 cells, as recommended

by ISO10993-5. Due to high cationic charge densities within the polymer structure, cytotoxic effects known from literature can be expected.[34, 35] As depicted in Figure 2, a concentration-dependent cytotoxicity of all polymers was observed after 24 h. The lowest cell viability was observed for the homo polymers **PD**, **PM** and **PA** as well as for the copolymer **PDM** revealing CC_{50} values (50% cytotoxic concentration) of 23 µg mL^{-1} for **PM** and 19 µg mL^{-1} for the remaining polymers. Whereas, the co- and terpolymers containing primary amino groups showed moderate cytotoxicities with CC_{50} values of 62 µg mL^{-1} (**PDA**), 38 µg mL^{-1} (**PMA**) and 31 µg mL^{-1} (**PDMA**), respectively. The CC_{50} values of the polymers, except **PDA**, are within the range of linear polyethylene imine (lPEI 25 kDa, CC_{50} = 25 µg mL^{-1}), which is the most prominent polymer-based vector used for gene delivery. The molar mass-dependent cytotoxicity of lPEI can be explained by its high cationic charge density. But it should be considered that the polymer-mediated gene delivery mostly correlates with the cytotoxicity of polyamines, which is the main issue in transfection.

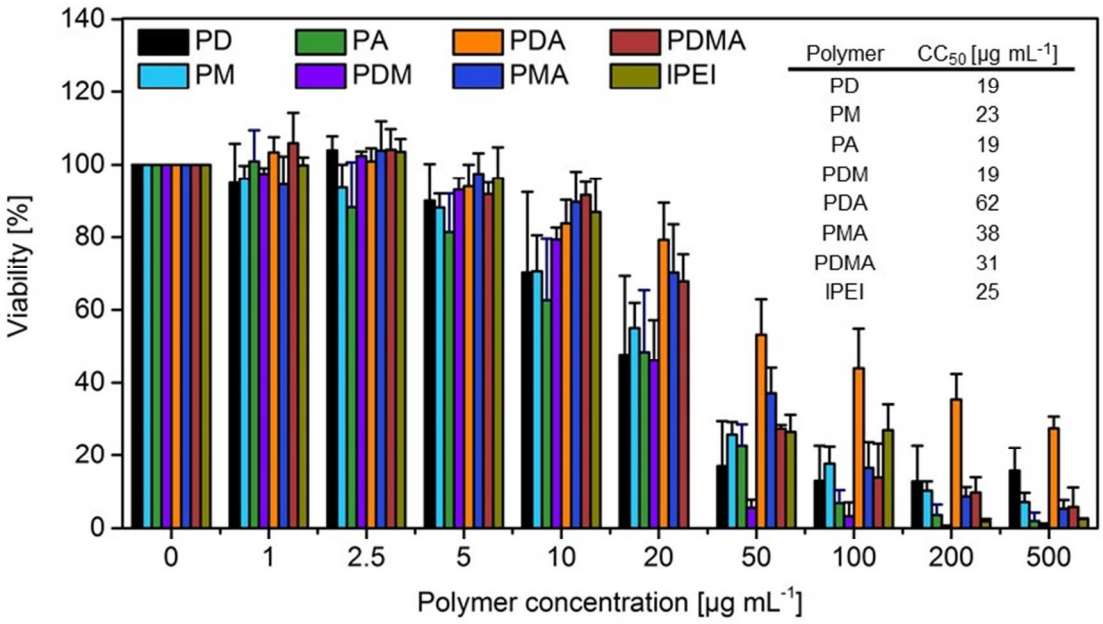

Figure 2. Cytotoxicity evaluation of the methacrylate-based homo- and copolymers **PA** to **PDMA** including lPEI 25 kDa (as control) at indicated concentrations after 24 h. CC_{50} values represented in the table were calculated applying the Boltzman fit (see Figure S7). Values represent the mean ± S.D. (n=3).

In addition to that, the membrane activity of the polymers was investigated using erythrocytes suspended in PBS (Figure 3 A and B). All polymers revealed a strong interaction with cellular membranes indicated by the increased hemolytic activity (Figure 3 A) and erythrocyte aggregation (Figure 3 B). The membrane activity was higher for polymers containing primary amino groups. As a significantly higher erythrocyte damage was observed at transfection relevant concentration (see values for 10 µg mL^{-1}). Membrane destabilization and rupture indicate a strong membrane activity resulting in a severe cytotoxicity.[13, 29]

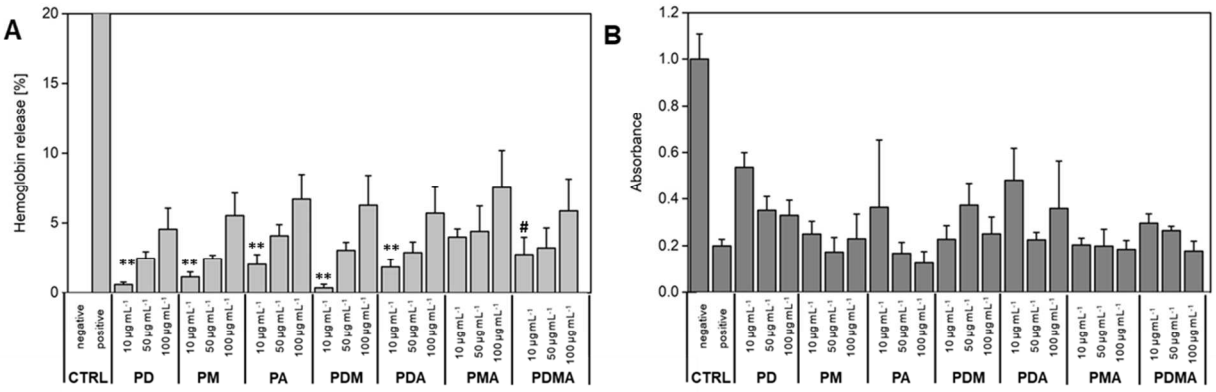

Figure 3. Hemocompatibility studies of metharcylate-based homo- and copolymers **PD** to **PDMA**. **(A)** Erythrocyte hemolysis assay of polymers at indicated concentrations. Triton X-100 served as positive control (99,8% hemolysis) and PBS as negative control (0%). A value less than 2% hemoglobin release was classified as non-hemolytic and values > 5% as hemolytic. T-test of the hemolysis values at 10 µg mL^{-1} in comparison to PMA; ** ≤ 0.005; # > 0.05. **(B)** Aggregation of erythrocytes after polymer treatment at indicated concentrations. PBS was used as negative control and bPEI (25 kDa) as postitive control. Values represent the mean ± S.D. (n=3).

Methacrylate-based polyplexes

In order to examine the binding affinity of all polymers to nucleic acids, the ethidium bromide quenching assay (EBA) was performed using pDNA (4.8 kb) as genetic material to be transfected.[36, 37] Different nitrogen (polymer) to phosphate (DNA) ratios (N/P) were used for the polyplex preparation in order to assess the optimal conditions for a stable polyplex formation. All tested polymers revealed the ability to

condense pDNA and to form polyplexes with increasing N/P ratios (Figure 4 A). This was indicated by the decrease in fluorescence intensities, as a result of the exclusion of ethidium bromide from its binding site within the pDNA. At higher N/P ratios (10 to 20) a plateau of constant fluorescence values is formed in all cases, which indicates a stable polyplex formation. However, the overall fluorescence intensities vary depending on the type of composition of the polymers. Homo- and copolymers based on DMAEMA (**PD**, **PDM**, **PDA**) displayed higher relative fluorescence intensities between 60 to 45%. Those polymers demonstrated only a reduced ability for pDNA condensation, which can be related to the sterically hindered tertiary amino groups. The presence of primary and secondary amino groups (**PM**, **PA**, **PMA** and **PDMA**) resulted in improved DNA condensation properties (fluorescence intensities below 40%). These observations clearly confirmed the trend for an improved DNA complexation by primary and secondary amino groups.[13, 28, 38]

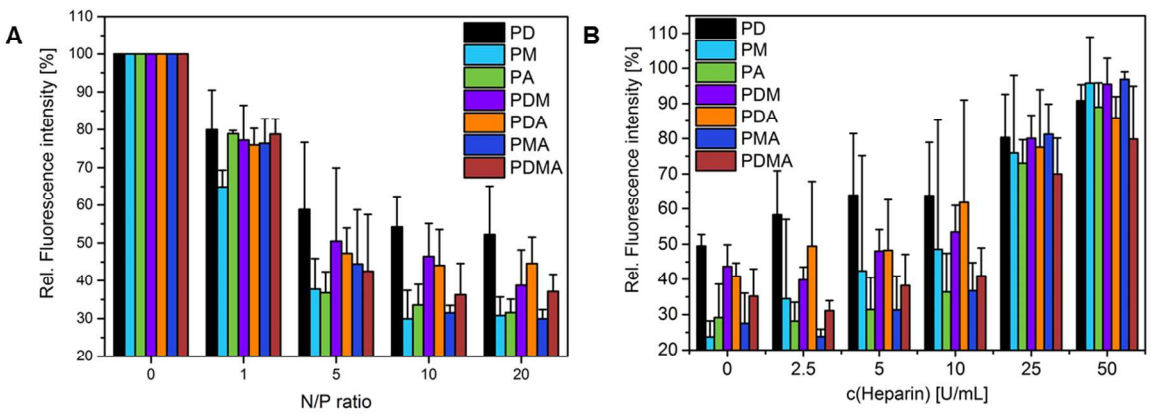

Figure 4. Polyplex stability: **(A)** Ethidium bromide quenching assay with polyplexes of **PD** to **PDMA** prepared at different N/P ratios (pDNA). **(B)** Dissociation assay of polyplexes **PD** to **PDMA** (N/P 20) using heparin at different concentrations. Values represent the mean ± S.D. (n=3).

Despite differences in the complexation behavior and the resulting relative fluorescence intensities, all polyplexes featured comparable sizes below 200 nm at N/P 20 with a high cationic surface charge between 35 to 39 mV (Table 3), which is typical for cationic methacrylates.[39-41] Nevertheless, the prepared polyplexes exhibited a broad size distribution as indicated by the relatively high PDI values. This fact indicates the presence of a disperse polyplex population and suggests the formation of aggregates, which

is a consequence of the preparation method as well as the used complexation buffer. The high dispersity is most likely caused by the preparation of polyplexes with higher N/P ratios than necessary for neutralization of the pDNA charges. However, this method (vigorous mixing of pDNA and polymer) is known to show improved polyplex stability and transfection performance.[42]

Table 3. Size and zeta potential of pDNA-polyplexes prepared with **PD** to **PDMA** at N/P 20.

Polyplexes of	Z-Average [d.nm]	PDI	ζ (Zeta potential) [mV]
PD	84	0.4	37
PM	97	0.4	37
PA	180	0.4	39
PDM	138	0.3	37
PDA	144	0.4	35
PMA	115	0.4	38
PDMA	148	0.3	39

Polyplexes were measured in 20 mM 4-(2-hydroxethyl) piperazine-1-ethanesulfonic acid (HEPES) and 5% (w/v) glucose, at pH 7.2 by dynamic and electrophoretic light scattering.

The dissociation capability of the genetic material from polymer was investigated by the heparin dissociation assay (Figure 4 B).[43] The previously formed polyplexes were treated with different concentrations of heparin to force the release of pDNA within the polymer complex as competitor to the polymer. Hence, ethidium bromide will be able to intercalate into the displaced nucleic acid once more, leading to an increase in fluorescence intensity. The tested methacrylate-based polymers seem to force a strong condensation of pDNA, since very high concentrations of heparin (50 U mL^{-1}) were required to reach a (almost) full release of the pDNA from the polyplexes. The swiftest release was achieved with **PD**, **PDM** and **PDA**, although such copolymers comprising DMAEMA units only revealed reduced pDNA dissociation rates (80 to 85%).

Polyplex performance

Since various studies reported good transfection efficiencies (TE) of methacrylate-based polymers or particles,[12, 44, 45] the transfection capability of the polymer library was evaluated at various conditions. For this purpose, HEK-293 cells were transfected with pDNA encoding the enhanced green fluorescence protein (EGFP). The transfection efficiency was determined by flow cytometry (Figure 5) analyzing all viable cells (counterstaining with propidium iodide, red) successfully expressing EGFP (green). Despite the fact that **PD** possessed the highest buffer capacity at slightly acidic conditions, which is thought to be beneficial for endosomal release, it demonstrated the lowest transfection levels (< 20% TE) at different N/P ratios independent of serum-reduced or serum-containing cell media. Similar observations were reported previously.[40, 46] The best transfection efficiencies were achieved with **PA** (66 %TE) and **PMA** (56% TE) revealing comparable gene expression to lPEI, the standard of transfection (25 kDa, Polyscience) at a N/P ratio of 20. The terpolymer **PDMA** showed also good transfection levels (43% TE) at N/P 20, while **PM**, **PDM** and **PDA** revealed moderate TEs between 20 and 30%. A concentration-dependent impairment of the overall cell viability during transfection in serum-reduced medium was observed (Figure S8) and showed similar tendencies compared to the cytotoxicity profile of polymers (see Figure 2). It has to be mentioned that the assessment of the viability by flow cytometry (PI staining) is based on membrane leakage and, therefore, not directly comparable to the alamarBlue assay. Nevertheless, it is known that polyplexes revealed decreased cytotoxicity compared to free polymers, as the cationic charge is partially masked upon complexation with nucleic acids.[47] In the presence of serum proteins, the intracellular level of EGFP decreases drastically, meaning maximum TEs below 20% for all methacrylate-based polymers as well as lPEI. Furthermore, improved cell viabilities for tested polyplexes at these conditions were observed (Figure S8). Due to their strong cationic character, negatively charged proteins may aggregate with the polyplexes, which causes an alteration in the surface charges and the sizes of the complex, finally leading to the formation of larger structures and the masking of the positive net charge.[48, 49] This effect in turn may lead to a reduced affinity to cell membranes (polymer-membrane interaction), diminished uptake of polyplexes and, consequently, to a reduction in transfection efficiencies.[50, 51]

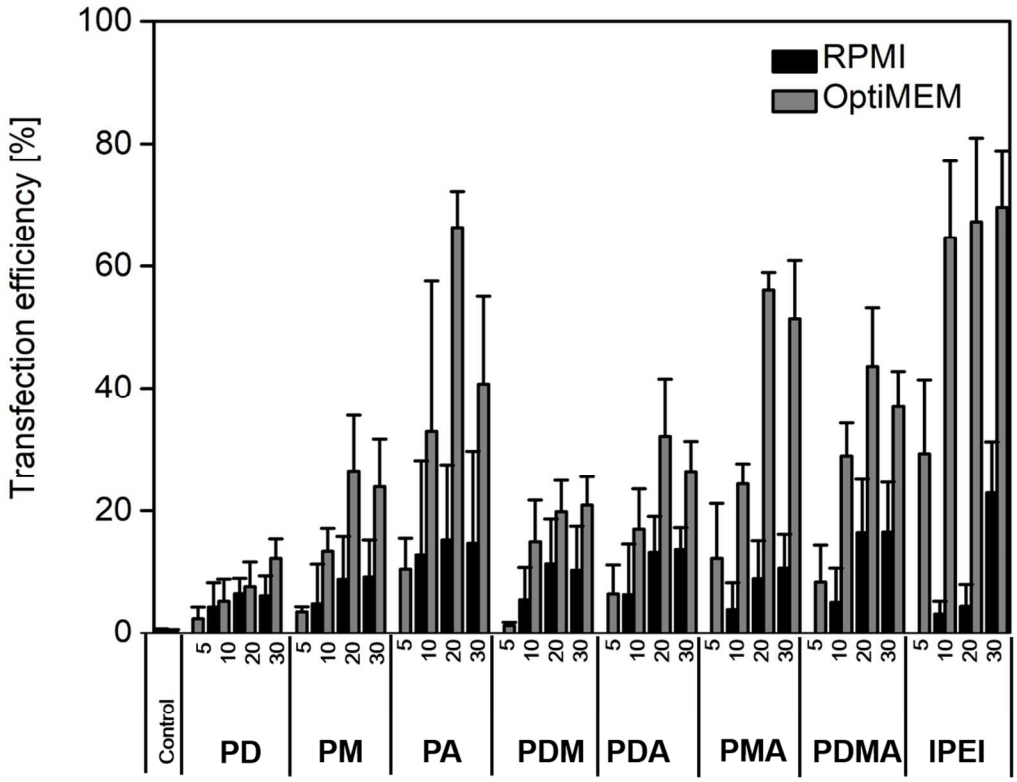

Figure 5. Transfection study of adherent HEK-293 cells in serum-reduced (OptiMEM, light grey) and serum-containing media (RPMI + 10% FCS, black) with all polymers of the library and commercial 25 kDa lPEI as positive control at different N/P ratios after 24 h. Values represent the mean ± S.D. (n=3).

Based on the results obtained from flow cytometry experiments, we conclude that polymers with tertiary amino groups and an average molar mass in the range of 20 kDa are not beneficial for transfection, whereas primary amino groups have a substantial impact on the successful delivery of nucleic acids, as the highest transfection efficiency was observed for the polymer with the highest primary amine content (serum-reduced conditions). It should be mentioned, that the transfection efficiency of PDMAEMA was previously shown to increase with the increase of the molar mass.[52] The best polymer for transfection was **PA**, which composes 100% AEMA units. Polymers including additional secondary amino groups (**PMA** and **PDMA**) also demonstrated improved outcomes compared to polymers without any primary amino groups. Homopolymers with 100 mol% tertiary or secondary amino groups as well as copolymers consisting of varying ratios of the corresponding monomers lacked the ability to efficiently transfect

HEK-293 cells. Despite the beneficial buffer capability based on the presence of tertiary amino groups, various studies have been questioning the endosomal escape mechanism of PDMAEMA by the proton sponge effect [16, 53, 54]. Our results further undermine this theory, since the buffer capacities of the methacrylate-based polymers do not correlate with their ability for gene expression.[55, 56]

To gain a deeper insight of the differences in the gene delivery performance of the methacrylates, we investigated the uptake behavior of the polyplexes. It has been reported that cationic polyplexes are internalized into cells by endocytosis.[57, 58] Since we obtained polyplexes with favorable sizes below 200 nm and cationic net charges, their cellular uptake was investigated by flow cytometry measurements using YOYO-1 labeled pDNA and bafilomycin, a vacuolar type H^+-ATPase inhibitor (see SI Figure S9 A and B). Uptake studies at 4 °C confirmed an energy-dependent internalization pathway *via* endocytosis, shown by the inhibition of the polyplex uptake into HEK-293 cells (Figure S9 A). Furthermore, results obtained by the treatment of cells with bafilomycin further support an uptake by endocytosis, since an almost complete inhibition of EGFP transfection was observed (Figure S9 B). This effect is caused by the inhibition of the acidification of endo-lysosomal organelles, which prevents the endosomal release of polyplexes into the cytoplasm and thus a successful transfection. This experiment further supports the requirement of polymer protonation through acidification to achieve sufficient endosomal escape.

In contrast, uptake studies at 37 °C revealed a time-dependent uptake of YOYO-1 labeled polyplexes, where about 80% of HEK-293 cells presented internalized polyplexes after 4 h (Figure 6 A). In particular, the homopolymers **PD** (MFI = 188) and **PA** (MFI = 159) followed by **PDM** (MFI ~ 150) revealed the highest amount of YOYO-1 positive cells.

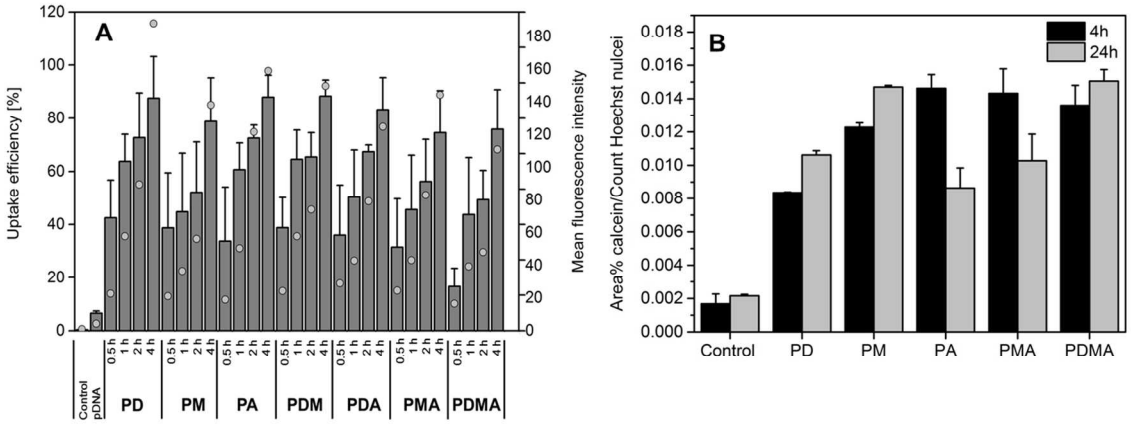

Figure 6. (A) Polyplex uptake of adherent HEK-293 cells in serum-reduced media using YOYO-1 labeled pDNA. The uptake efficiency (columns) and the mean fluorescence intensity of all viable cells (dots) measured by flow cytometry after certain time points. Values represent the mean ± S.D. (n=3). **(B)** Quantification of endosomal release by the calcein quenching assay. HEK-293 cells were treated with **PD**, **PM**, **PA**, **PMA** and **PDMA** polyplexes and simultaneous supplementation of calcein (25 µM). After 4 h and 24 h the endosomal release of polyplexes was evaluated by the release of calcein from endosomes into the cytoplasm of the cells, leading to high fluorescence signals. Ratio of green fluorescent calcein area in % over the number of detected Hoechst stained nuclei in HEK-293 cells were detected by fluorescence microscopy and quantified using ImageJ.

Our results indicate that a high uptake is not the limiting step for high transfection levels,[59] since the endosomal release represents a further critical hindrance in the gene delivery process.[29, 60] Therefore, the endosomal escape of the homopolymers **PD**, **PM** and **PA** as well as the best performing copolymer **PMA** and terpolymer **PDMA** was further examined *via* a calcein quenching assay after 4 and 24 h (see Figure 6 B and SI Figure S10 and S11). Calcein is a membrane impermeable fluorophore, which is not able to enter cells by diffusion, but by fluid-phase endocytosis. As calcein is, therefore, trapped within the endo-lysosomes, it can only escape by membrane disruption, which leads to a bright fluorescence in the cytosol by the distribution of calcein throughout the whole cell.[54, 61] Since our polymers and polyplexes revealed increased interaction with cellular membranes (see hemolysis and aggregation data), they may promote the release of calcein from endo-lysosomes within the cytoplasm compared to untreated cells. This experimental setup is designed to model the potential release mechanisms hypothesized by earlier studies

on methacrylates with artificial membranes.[15] Representative images of HEK-293 cells with calcein remaining captured within the endo-lysosomes (control) as well as images of successfully released calcein (**PMA**) are provided within the Supporting Information (Figure S10 and S11). After endosomal release of the dye into the cytosol, the fluorescent area of the calcein signal should increase while the relative fluorescence intensity should decrease in comparison to the stained cell nuclei. The evaluation of the endosomal release was done by image analysis of the captured fluorescence pictures using the ImageJ software as described in the experimental section focusing on the increase in relative fluorescent area to the number of stained nuclei. The differentiation between endosomal and cytosolic fluorescence was limited using fluorescence microscopy regarding spatial information and resolution quality. Therefore the overall fluorescent area was plotted against the number of Hoechst stained nuclei. The results revealed an increased fluorescent area of HEK-293 cells treated with methacrylate-based polyplexes compared to cells treated only with calcein (control). The methacrylate-based polyplexes showed a up to eight-times higher relative fluorescent area after 4 h in contrast to the control**,** which represents a hint for an early endosomal escape by membrane disruptive activity. In particular, **PA**, **PMA** and **PDMA** showed the fastest endosomal release, whereas **PD** revealed a lower ratio of escape after 4 h. This trend may relate to its poor transfection performance. **PD** seems to be unable to escape the endosomes in a time efficient manner as for instance **PA**, thus being kept entrapped within endo-lysosomes despite its high buffer capacity. As mentioned earlier, various studies have been questioning the endosomal escape of PDMAEMA by the proton sponge effect [16, 53, 54]. For example, Jones *et al.* reported the lack of an endosome disruptive activity of PDMAEMA as an explanation for its diminished transfection performance.[54] After 24 h, the fluorescence area of **PA** and **PMA** treated cells decreases compared to the other measured polyplexes, which indicates a fast release within few hours. A decrease in calcein fluorescence intensity after 4 h was also reported by others and explained by the activity of P-glycoprotein pumps, which might transport calcein out of the cell.[62] A rapid endosomal release of polyplexes within the first hours during the transfection process seems to correlate with high transfection efficiency, as the highest transfection levels were observed for **PA** and **PMA**.

In order to elucidate the location and membrane interaction of the polyplexes, high-angle annular dark-field scanning transmission electron microscopy (HAADF-STEM) was applied. This method provides a resolution down to a few nanometers and combines it with the capability to reveal the ultrastructure of the cellular interior. Figure 7 shows representative images of HEK-293 cells, embedded into an Epon-based resin, after exposure to polyplexes based on **PMA** for 4 h incubation time. In addition to the cellular organelle structures (*i.e.* mitochondria, vesicles, nucleus), structures of high electron density (dark/black) were observed. We attribute these structures to polymer-DNA complexes, since the functional groups of the polyplex (amines and phosphates) exhibit a strong chemical affinity to the standard staining reagents (OsO_4 and uranyl acetate) resulting in an efficient staining of polyplexes. This staining ability of mentioned reagents has been observed for a variety of different polyplexes so far.[63] In Figure 7 A and B, **PMA** polyplexes are located within endosomal structures and partially a high number of polyplexes is observed within these structures. In the periphery of the cells the formation of aggregates is evident (red arrow), however, also smaller aggregates are observed to approach the cells. Next to completely filled endosomal structures some intracellular vesicles are filled with a low number of densely packed polyplexes alongside a large amount of intracellular fluids. In Figure 7 B an increased interaction of the polyplexes with the endosomal membrane is observed in some cases (yellow arrows), which can be explained by the electrostatic interaction between the positively charged polyplexes and the negatively charged membranes. A close vicinity of the polyplexes to the endosomal membrane was also observed for PEI-based polyplexes.[64] Moreover, in some cases alterations of the endosomal membrane structures become evident. Here, the polyplexes are partially observed in close vicinity to the endosomal structure, which are associated with deformed membranes (green arrows). These structural changes can be attributed to endosomal escape events. An alternative escape strategy to the proton sponge effect might be induced by the direct interaction of methacrylate-based polyplexes with the endo-lysosomal membrane causing a membrane destabilization and a subsequent release due to pore formation without complete rupture. This effect was previously reported for cationic polymers.[59, 60, 65-67] A disturbed membrane integrity of polyplex-containing vesicles was observed, as parts of the electron dense structures were detected outside

of the vesicular membrane and reaching into the cytoplasm of HEK-293 cells (indicated by red arrow heads). This observation, as well as our previous results (hemolysis and calcein assay), support an endosomal escape by hole-formation due to an increased tension on the membrane rather than a complete osmotic rupture of the endosome.

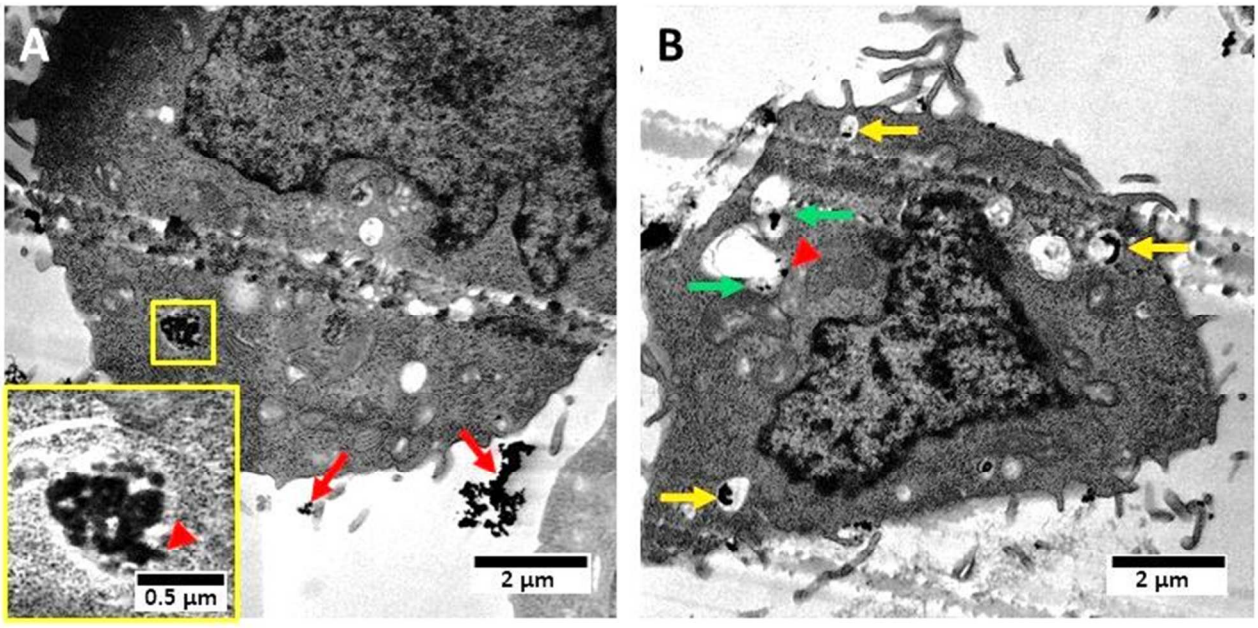

Figure 7. HAADF-STEM images of polyplex treated HEK-293 cells for 4 h in OptiMEM. Polyplexes can be observed as electron dense structures (black). **(A-B) PMA** polyplex treated cells: Red arrows indicate polyplex aggregation in the extracellular environment. Yellow arrows indicate interaction of polyplexes with the membrane of endo-lysosomal vesicles. Green arrows indicate deformed membrane structures of endo-lysosomes caused by polylpex interaction. Red arrowheads indicated disturbed membrane integrity of polyplex-containing vesicles and potential membrane disruption or pore formation. Polyplex structures (black) seems to pass from endosomes to cytoplasm.

CONCLUSION

In an effort to understand the influence of different amino functionalities in methacrylate-based polymers on their transfection efficiency, we have synthesized a library of defined linear homo- and copolymers bearing primary, secondary and tertiary amino groups. The polymers were prepared using the RAFT process and revealed similar molar masses with a DP of 163 to 250 and narrow dispersities (Đ= 1.09 to 1.28) as well as varying compositions of DMAEMA, MAEMA and AEMA monomers. pK_a values between 7.45 and 8.40 were observed, leading to a partially protonation of all polymers at physiological conditions. The buffer capacities, in particular for **PD**, are in the pH range of endosomal environments, which is supposed to be beneficial for transfection. All synthesized polymers were able to bind and condense pDNA resulting in the formation of stable, nanosized polyplexes (< 200 nm). Furthermore, the performance of these polymers as gene delivery vehicles was examined at different conditions by microscopic techniques (fluorescence and scanning transmission electron microscopy) as well as flow cytometry measurements. It was found that several parameters (Figure 8) show a relevant impact on the successful transfection: Most importantly (i) the type and content of the amino group, (ii) the interaction of the polymer with the membrane and (iii) a rapid endosomal release. However, the size of polyplexes, their uptake rate and interestingly, the buffer capacity revealed no direct correlation with the observed transfection levels. Based on our results, the transfection efficiency of such polymers can be summarized regarding their amino functionalities as the following: Primary amino groups > Secondary amino groups > Tertiary amino groups. High contents of primary amino groups in homo- (**PA**) and copolymers (**PMA**) resulted in an improved transfection efficiency, whereas higher amounts of tertiary amino groups within the polymer structure seem to hamper the transfection process (**PD** and **PDM**). A primary amino content of at least ~ 40 to 50 mol% was found to be necessary for efficient transfection, since already the copolymer **PDA** ($AEMA_{30\%}$-$DMAEMA_{70\%}$) comprising ~70 mol% of tertiary amino groups showed reduced results. With the addition of 30 mol% secondary amino groups, the transfection performance of the terpolymer **PDMA** ($AEMA_{30\%}$-$MAEMA_{30\%}$-$DMAEM_{40\%}$) in contrast, significantly increased compared to **PDA**. This effect was only observed for copolymers of MAEMA, since the homopolymer

PM also demonstrated reduced transfection levels. The good performance of the presented homo- and copolymers could furthermore be explained by a strong polymer-membrane interaction rather than by a rupture mediated by osmotic swelling, as it is postulated for the proton sponge effect. However, it is demonstrated that the endosomal acidification is still required for further protonation of the polymers and therefore for their sufficient interaction with the endo-lysosomal membrane (see bafilomycin treatment). In fact, all polymers exhibited high hemoglobin release and erythrocyte aggregation, indicating their ability to destabilize membranes and to cause a partial rupture. Despite the fact that such a high membrane interaction leads to an increased cytotoxicity, this property seemed to be beneficial for a fast endosomal release. This assumption is in accordance to the results of our calcein quenching assay, which revealed a fast endosomal escape, in particular for **PA** and **PMA**. Based on this investigations, we conclude that the mechanisms for endosomal escape during transfection of methacrylate based polymers differ significantly from PEI, as they are unaffected by the respective buffer capacity and support the theory of the disruptive formation of pores.

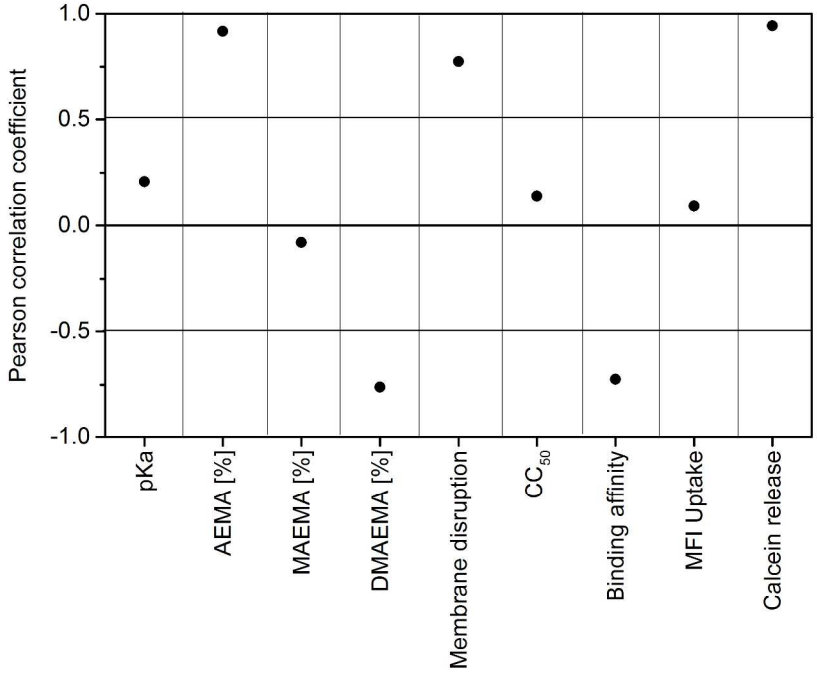

Figure 8. Overview of factors (main polyplex properties) with impact on the transfection efficiency using the Pearson correlation coefficient. Highest proportional correlation is represented by 1.0, whereas −1.0 means the highest invers proportional correlation. Values around zero indicate no correlation. For membrane disruption, the hemoglobin release at 10 μg mL^{-1} polymer concentration was used. For cytotoxicity the half maximum (50%) critical concentration (CC_{50}) was used. The binding affinity represents the measured relative fluorescence of ethidium bromide at N/P 20. To compare the mean fluorescence intensity (MFI) of polyplex uptake, the time (min) that was needed to reach 100 relative MFI (where the control is 1) was determined. The calcein release represents the ratio of green fluorescent calcein area in % over the number of detected Hoechst stained nuclei of the polymers after 4 h.

EXPERIMENTAL

Materials

Unless otherwise stated, the chemical were used without further purification. 2-(*N,N*-Dimethylamino)ethyl methacrylate (DMAEMA), methacryloyl chloride, anhydrous triethylamine, 4-cyano-4-(phenylcarbonothioylthio) pentanoic acid (CPDB-COOH), neutral aluminium oxide and 2-(methylamino)ethanol, propidium iodide and calcein were purchased from Sigma Aldrich (Merck). The inhibitor removal for DMAEMA was performed using the inhibitor remover from Sigma Aldrich. Linear and branched poly(ethylene imine) (lPEI/bPEI, 25 kDa) was obtained from Polyscience. Di-*tert*-butyldicarbonate for the protection was from Alfa Aesar and 2-aminoethanol was purchased by TCI. 2-Bisazobutyronitile was received from Acros and recrystallized from methanol prior to use. Hydrochloric acid, dimethylformamide and tetrahydrofurane were purchased from VWR Chemicals, all other solvents used were obtained from standard suppliers. Ethidium bromide solution (1%, 10 mg mL^{-1}) was obtained from Carl Roth. AlamarBlue, YOYO-1 iodide and Hoechst 33342 (10 mg mL-1 solution) were obtained from Life Technologies (Thermo Fisher). If not stated otherwise, cell culture consumables, cell culture media and supplements (L-Glutamin, antibiotics) were obtained from Greiner Bio-One, Lonza and Biochrom (Merck Millipore), respectively. Plasmid pEGFP-N1 (4.7 kb, Clontech, USA) encoding green fluorescent protein (EGFP) was isolated with the Giga Plasmid Kit provided by Qiagen. Double-stranded DNA (dsDNA, 23 nucleotides) was purchased from Jena Bioscience.

Synthesis of *N-tert*-butyloxycarbonyl-(2-aminoethyl)-methacrylate (BocAEMA)

N-tert-Butyloxycarbonyl-(2-aminoethyl)-methacrylate was synthesized according to a procedure of Kuroda et al..[24] 10 g of 2-Aminoethanol were dissolved in 120 mL THF and 200 mL of a 1 M aqueous sodium hydroxide solution were added. 35.28 g of di-*tert*-butyldicarbonate in 80 mL THF were added dropwise while cooling the reaction mixture in an ice bath and stirred overnight. The mixture was diluted with ethyl acetate and washed with water, $NaHCO_3$ and brine and the aqueous phase was reextracted with ethyl acetate, dried over sodium sulfate and the solvent was removed under reduced pressure. Without

further purification 18.5 g of *N-tert*-butyloxycarbonyl-2-aminoethanole was diluted with 30 mL dry dichloromethane under schlenk conditions and 22.6 mL of dry triethylamine was added while cooling the mixture in an ice bath. 15 mL Methacryloylchloride were added dropwise and the reaction was stirred overnight. The mixture was washed with water, brine and sodium hydrogen carbonate and dried over sodium sulfate. The crude off white product was finally recrystallized from *n*-hexane.^{1}H NMR (300 MHz, $CDCl_3$): δ [ppm] = 1.42 (s, 9H), 1.93 (s, 3H), 3.43 (m, 2H), 4.18 (t, 2H), 4.8 (br. s, 1H), 5.57 (s, 1H), 6.10 (s, 1H). ^{13}C NMR (75 MHz, $CDCl_3$): δ [ppm] = 18.2 (CH3), 28.3 (CH3), 39.6 (CH2), 63.9 (CH2), 79.5(CH2), 125.8 (Cquart), 136.0 (Cquart), 155.7 (Cquart), 167.2 (Cquart).

Synthesis of *N*-methyl-*N-tert*-butyloxycarbonyl-(2-aminoethyl)-methacrylate (BocMAEMA)

N-Methyl-*N-tert*-butyloxycarbonyl-(2-aminoethyl)-methacrylate was synthesized according to a procedure of Sinclair *et al.*[25]. 10 g *N*-Methylaminoethanol was dissolved in 80 mL chloroform was cooled in an ice bath and 29 g di-*tert*-butylcarbonate in 80 mL was added dropwise and stirred at room temperature for 1 h. The solvent was removed under reduced pressure and the mixture was purified by distillation (30 mbar, 180 °C). Under schlenk conditions 21.4 g of *N*-methyl-*N-tert*-butyloxycarbonyl-2-aminoethanol were diluted with 100 mL dry dichloromethane, 49.4 mL triethylamine was added and the reaction mixture cooled in an ice bath. 17.7 mL methacryloyl chloride in 100 mL dichloromethane were added dropwise and the reaction was stirred at room temperature overnight. The mixture was washed with water and brine and dried over sodium sulfate. Further purification was done by column chromatography using a mixture of cyclohexane an ethyl acetate (9:1-3:1).^{1}H NMR (300 MHz, $CDCl_3$): δ [ppm] = 1.96 (s, 9H), 2.76 (m, 3H), 3.30 (m, 2H), 4.56 (m, 2H), 5.65 (s, 1H), 6.30 (s, 1H). ^{13}C NMR (75 MHz, $CDCl_3$): δ [ppm] = 18.2 (CH_3), 28.3 (CH_3), 35.2 (CH_2), 47.9 (CH_3), 62.7 (CH_2), 79.7(CH_2), 126.0 (C_{quart}), 136.1 (C_{quart}), 155.8 (C_{quart}), 167.1 (C_{quart}).

Synthesis of homo- and copolymers

Homo- and copolymers of BocAEMA, BocMAEMA and DMAEMA were prepared by the reversible addition-fragmentation chain transfer (RAFT) polymerization method.[10] In a typical RAFT

copolymerization experiment, 0.735 g of BocAEMA (3.18 10^{-3} mol), 0,773 g of BocMAEMA (3.18 10^{-3} mol), 0.98 mg of AIBN initiator (5.96 10^{-5} mol), 5.68 mg of CPDB-COOH RAFT agent (20.33 10^{-5} mol) and 5.03 mL DMF were mixed together with anisole as internal standard (0.347 mL) in a 25 mL reaction vial. The monomer concentration was kept at 1 mol L^{-1}. The reaction mixture was degassed with argon for at least 30 min and subsequently, the reaction solution was placed in a preheated oil bath at 70 °C for 38 h. The copolymer was purified by two times precipitation from THF into a minimum of 10-fold amount large volume of *n*-hexane and dried under reduced pressure. Conversion was measured by ^{1}H-NMR spectroscopy using anisole as internal standard.

The RAFT polymerization of the DMAEMA homopolymers was carried out in ethanol in 1.73 molar solution. 1.572 g DMAEMA (0.01 mol), 2.8 mg 4,4′-azobis(4-cyanovaleric acid) (0.001 mmol) and 11.1 mg 4-cyano-4(pehnylcarbonthiothioylthio) pentanoic acid (0.004 mmol) were dissolved in 3.3 mL of ethanol and 0.77 mL DMF were added as internal standard. The reaction mixture was degassed with argon for 10 min and heated to 70 °C for 10 h. The resulting polymer was purified *via* precipitation from THF in *n*-hexane twice and dried at high vacuum. Conversion was measured by ^{1}H-NMR

Deprotection of Boc-protected polymers

Boc-protected homo- and copolymers were deprotected using diluted hydrochloric acid in methanol. In a typical procedure, 300 mg polymer was dissolved in 10 mL methanol and 1 mL of concentrated hydrochloric acid was added dropwise and stirred at room temperature overnight. The solvent was removed under reduced pressure, dissolved in water and freeze dried.

Asymmetric flow field-flow fractionation (AF4)

Asymmetric flow field-flow fractionation (AF4) was performed on an AF2000 MT system (Postnova Analytics, Landberg, Germany) coupled to an UV (PN3211, 260 nm), RI (PN3150), MALLS (PN3070, 633 nm) detector. The eluent is delivered by two different pumps (tip and focus-flow) and the sample is injected by an autosampler (PN5300) into the channel. The channel has a trapezoidal geometry and an

overall area of 31.6 cm². The nominal height of the spacer was 500 µm and a regenerated cellulose membrane with a molar mass cut-off of 10,000 g mol^{-1} was used as the accumulation wall. All experiments were carried out at 25 °C and the eluent was 20 mM NaCl in 25 mM sodium acetate buffer at pH 3.5. The detector flow rate was set to 0.5 mL min^{-1} for all samples and a sample volume of 50 µL (10 mg mL^{-1}) were injected with an injection flow rate of 0.2 mL min^{-1} for 7 min. For all samples the cross-flow was set to 2 mL min^{-1}. After the focusing period and a transition time of 1 min, the cross flow was kept constant for 1 min and then decreased under a power function gradient 0.40 to zero within 15 min. Afterwards the cross-flow was kept constant at zero for 20 min to ensure complete elution. For calculation of the molar mass a Zimm plot was used. The refractive index increment (dn/dc) of all samples was measured by manual injection of a known concentration directly into the channel without any focusing or cross-flow. The dn/dc was calculated as the average of at least three injections from the area under the RI curve.

NMR spectrometry

NMR spectra were recorded on a Bruker AC 300 MHz or on a Bruker AC 250 MHz spectrometer.

Titration

The titration for the detection of the pK_a value of the polymers was performed with the automated titrator 765 Dosimat (Metrohm, Herisau, Swiss) and the pH detector GMH3530 (GHM Messtechnik GmbH Standort Greisinger, Regenstauf, Germany). For a typical measurement the polymer in ultrapure water (10 mg mL^{-1}) was acidified by 10 µL hydrochloric acid and stirred while titrated against a 0.1 M sodium hydroxide solution (0.1 mL min^{-1}) to a pH value of 12. The pK_a value was using the Henderson-Hasselbalch equation (2) by determining the equivalence point from the titration diagram.

$$pH = pK_a + log\frac{[A^-]}{[HA]} \qquad (2)$$

Size exclusion chromatography (SEC)

Size exclusion chromatography (SEC) was measured on a Agilent 1200 series system equipped with a PSS degasser, a G1310A pump, a G1362A refractive index detector and a PSS GRAM guard column running with dimethylacetamide (DmAc) with 0.21 % of lithium chloride. The Techlab oven was set to 50 °C and the molar masses were calculated using a poly(methyl methacrylate) (PMMA) standard. For the water soluble polymers a SEC system of Jasco was used with a DG-980-50 degasser, a PU-980 pump, equipped with a RI-930 RI detector and Jasco oven set to 50 °C. The column used was AppliChrom ABOA CatPhil, which is operated with a water solution with 0.1 % trifluoric acid and 0.1 M NaCl.

Polyplex preparation

Polyplexes of plasmid DNA (pDNA) and polymers were prepared by mixing stock solutions of 15 μg mL^{-1} pDNA and different amounts of polymers (1 mg mL^{-1}) to obtain various N/P ratios (nitrogen of polymer to phosphate of pDNA) in HBG buffer (20 mM 4-(2-hydroxethyl) piperazine-1-ethanesulfonic acid (HEPES) and 5% (w/v) glucose, pH 7.2). The solutions were vortexed for 10 sec at maximal speed and incubated at room temperature for 15 min to ensure complex formation.

Ethidium bromide quenching assay

The formation of polyplexes with pDNA was examined by quenching of the ethidium bromide fluorescence. Briefly, 15 μg mL^{-1} pDNA in a total volume of 100 μL HBG buffer were incubated with ethidium bromide (0.4 μg mL^{-1}) for 10 min at room temperature. Subsequently, polyplexes with different amounts of polymer (various N/P ratios) were prepared in black 96-well plates (Nunc Thermo Fisher) and incubated at room temperature for 15 min before the fluorescence measurements. The fluorescence of the samples was measured at an excitation wavelength of 525 nm and an emission wavelength of 605 nm using a Tecan microplate reader. A sample containing only pDNA and ethidium bromide was used to calibrate the device to 100% fluorescence against a background of 0.4 μg mL^{-1} of ethidium bromide in HBG solution. The percentage of dye displaced upon polyplex formation was calculated using equation (3):

$$\text{RFU}\ [\%] = \frac{F_{sample} - F_0}{F_{pDNA} - F_0} * 100 \qquad (3)$$

Here, RFU is the relative fluorescence and F_{sample}, F_0, and F_{pDNA} represents the fluorescence intensities of a given sample, the ethidium bromide in HBG alone, and the ethidium bromide intercalated into pDNA alone.

Heparin dissociation assay

Polyplexes with an N/P ratio of 20 were prepared as described above in a total volume of 100 µL HBG buffer containing ethidium bromide (0.4 µg mL^{-1}). After incubation in the dark at room temperature for 15 min, polyplexes were transferred into a black 96-well plate, and heparin of indicated concentrations were added. The solution was mixed and incubated for further 30 min at 37 °C in the dark. The fluorescence of ethidium bromide was measured at Ex 525 nm/Em 605 nm with a Tecan microplate reader. The percentage of intercalated ethidium bromide was calculated as described before.

Dynamic and electrophoretic light scattering

Dynamic light scattering (DLS) was performed on a Zetasizer Nano ZS (Malvern Insturments, Herrenberg) with a He-Ne laser operating at a wavelength of λ = 633 nm. All measurements (30 runs, triplicate) were carried out at 25 °C after an equilibration time of 120 sec. The counts were detected at an angle of 173°. The mean particle size was approximated as the effective (z-average) diameter and the width of the distribution as the polydispersity index of the particles (PDI) obtained by the cumulants method assuming a spherical shape. Electrophoretic light scattering (ELS) was used to measure the zeta potential (ζ). The measurement was performed on a Zetasizer Nano ZS (Malvern Instruments, Herrenberg, Germany) by applying laser Doppler velocimetry. For each measurement, 20 runs were carried out using the slow-field reversal and the fast-field reversal mode at 150 V. Each experiment was performed in

triplicate a 25 °C. The zeta potential was calculated from the electrophoretic mobility (μ) according to the Henry Equation. Henry coefficient f(ka) was calculated according to Oshima. For size determination of polyplexes a pDNA concentration of 15 μg mL^{-1} was used for preparation at N/P 20 in HBG buffer.

Determination of cytotoxicity

Cytotoxicity studies were performed with the mouse fibroblast cell line L929 (CCL-1, ATCC), as recommended by ISO10993-5. The cells were cultured in Dulbecco's modified eagle's medium (DMEM, Biochrom) supplemented with 10% fetal calf serum (FCS), 100 U mL^{-1} penicillin and 100 μg mL^{-1} streptomycin at 37 °C in a humidified 5% (v/v) CO_2 atmosphere. In detail, cells were seeded at 10^4 cells per well in a 96-well plate and incubated for 24 h. Afterwards, the testing substances (polymers) at different concentrations, ranging from 1 μg mL^{-1} to 500 μg mL^{-1}, were added to the cells and the plates were incubated for further 24 h. Subsequently, the medium was replaced by a mixture of fresh culture medium and alamarBlue solution, prepared according to the manufacturer's instructions. After a further incubation of 4 h at 37 °C, the fluorescence was measured at Ex 570 nm/Em 610 nm, with untreated cells on the same well plate serving as negative controls. The negative control was standardized as 0% of metabolism inhibition and referred as 100% viability. Data are expressed as mean ± SD of three independent determinations.

Hemolysis assay

The interaction of polymers with cellular membranes was examined by analyzing the release of hemoglobin from erythrocytes. Blood from sheep, collected in heparinized tubes, were provided by the Institute of Animal Science and Animal Welfare, Friedrich Schiller University Jena. The blood was centrifuged at 4,500 × g for 5 min, and the pellet was washed three times with cold 1.5 mM phosphate buffered saline (PBS, pH 7.4). After dilution with PBS in a ratio of 1:7, aliquots of erythrocyte suspension were mixed 1:1 with the polymer solution and incubated in a water bath at 37 °C for 60 min. After centrifugation at 2,400 × g for 5 min, the hemoglobin release into the supernatant was determined spectrophotometrically using a microplate reader at 544 nm wavelength. Complete hemolysis (100%) was

achieved using 1% Triton X-100 serving as positive control. Pure PBS was used as negative control (0% hemolysis). The haemolytic activity of the polycations was calculated as follow (4):

$$\% \text{ Hemolysis} = 100 * \frac{(A_{Sample} - A_{Negative\ control})}{A_{Positive\ control}} \quad (4)$$

A value less than 2% hemolysis rate were classified as non-hemolytic, 2 to 5% as slightly hemolytic and values >5% as hemolytic. Experiments were run in triplicates and were performed with three different blood donors.

Erythrocyte aggregation

Erythrocytes were isolated as described above. The erythrocyte suspension was mixed 1:1 with the polymer solutions (100 µL total volume) in a clear flat bottomed 96-well plate. The cells were incubated at 37 °C for 2 h, and the absorbance was measured at 645 nm in a microplate reader. Cells, which were treated with PBS served as negative control and 25 kDa bPEI (50 µg mL^{-1}, Sigma Aldrich) was used as positive control. Absorbance values of the test solutions lower than the negative control were regarded as aggregation. Experiments were runs in triplicates and were performed with three different donor bloods from sheep.

Polyplex uptake

HEK-293 cells (CRL-1573, ATCC) were routinely cultured in RPMI 1640 medium supplemented with 10% FCS, 100 µg mL^{-1} streptomycin, 100 IU mL^{-1} penicillin and 2 mM L-glutamine at 37 °C in a humidified 5% (v/v) CO_2 atmosphere.

For kinetic uptake studies of polyplexes, cells were seeded at a density of 10^5 cells per mL in 24-well plates and cultured for 24 h. One hour prior to the addition of polyplexes, the medium was changed to OptiMEM (Thermo Fisher). The pDNA was labeled with YOYO-1 iodide prior to polyplex preparation. For labeling of 1 µg pDNA, 0.026 µL of 1M YOYO-1 solution was mixed with pDNA and incubated for 15 min at 4 °C protected from light. Afterwards HBG buffer and polymers were added at the indicated

N/P ratio and polyplexes were formed as described previously. At least 50 µL polyplexes in solution were added to the cells. The cells were harvested 0.5, 1, 2, 4 and 24 h after polyplex addition and 10% trypan blue was added to quench the outer fluorescence of cells. For energy-dependent uptake studies, cells were equilibrated in OptiMEM at 4 °C 30 min prior polyplex addition. The plates were further incubated at 4 °C for 4 h. To determine the relative uptake of polyplexes, 10^4 cells were measured by flow cytometry using a Cytomics FC 500 (Beckman Coulter) and the amount of viable cells (propidium iodide counterstaining, red) showing YOYO-1 signal (green) were gated.

Calcein assay

Endosomal escape was evaluated by the calcein quenching assay, as reported earlier using dsDNA (Jena Bioscience) for polyplex preparation.[61] The calcein solution (25 µM final concentration, dissolved in ultrapure water) and polyplexes (N/P 20, 50 µL) were simultaneously added to HEK-293 cells supplemented in OptiMEM for 4 h. Subsequently, cells were washed three times with PBS to remove remaining calcein and free polyplexes. 250 µL phenol-free growth medium supplemented with Hoechst 33342 (1:1000) was added to cells for a further incubation period of 20 min prior to imaging analysis. To examine calcein release after 24 h, cells were cultured in fresh growth media without calcein after the washing steps for further 20 h. Imaging was performed with a fluorescence microscope (Axio Observer Z1, Carl Zeiss, Jena, Germany) equipped with a mercury arc UV lamp and the appropriate filter combinations for excitation and detection of emission (Hoechst 33342: Ex 405 nm/BP 435-490 nm; Calcein: Ex 458 nm/BP 510-550 nm). Five images of random well plate localizations per sample were captured with a Plan-Apochromat 10× 0.45 air objective while identical instrument settings (camera gain, integration time, UV lamp power). Image analysis was performed with the free available ImageJ software. Therefore, the images of Hoechst counterstained cell nuclei were processed using the ‘subtract background’ command (10 pixels, separate colors). Afterwards the ‘threshold’ was set using the ‘Otsu’ method in black and white (color space HSB, dark background) and the brightness was set to 5/255. The image type was set to 8-bit and converted ‘to Mask’ and the ‘watershed’ method was applied to avoid

overlapping of the cell nuclei by an automated manner. Finally the 'analyze particles' option was used (21-infinity pixel units, circularity 0.5-1.0, show outlines, display results, exclude edges and summarize) for particle counting of the cell nuclei. For the calcein images, the analysis was performed in the same manner, but instead of the 'watershed' method, the 'dilate' method was used. For determination of fluorescent area the 'analyze particles' protocol (0 to infinity pixels, circularity 0 to 1.0 and no outlines) was applied.

Transfection of adherent cells

For transfection studies, cells were seeded at a density of 10^5 cells per mL in 24-well plates and incubated for 24 h at 37 °C, 5% CO_2. One hour prior to transfection, cells were supplemented with 0.5 mL OptiMEM or fresh serum containing growth medium. Polyplexes were prepared as described above, and were added to the cells (50 µL per well). After an incubation time of 4 h at 37 °C, the supernatant was replaced by fresh growth medium and the cells were further incubated for 20 h. For analysis *via* flow cytometry (Cytomics FC 500, Beckman Coulter), cells were harvested by trypsinization. Dead cells were identified *via* counterstaining with propidium iodide. For determination of transfection efficiency, 10^4 viable cells expressing EGFP (green) were gated. The experiments were performed independently three times.

Transmission electron microscopy

For electron microscopy investigations, HEK-293 cells were seeded on 6-well plates with a cell density of 2×10^6 cells·mL^{-1} and incubated them with the respective polyplex (N/P 20) in OptiMEM for 4 h. Subsequently, cells were detached with trypsin and the resulting cell suspension was centrifuged, washed (PBS 1X) and fixed for 2 h with glutaraldehyde (2% in PBS 1X, prepared from 8% EM grade stock solution, purchased from EMS, Hatfield) on ice. After glutaraldehyde fixation, the cells were again washed with PBS and postfixed with osmium tetroxide (1% in PBS, prepared from 4% EM grade stock solution, purchased from EMS, Hatfield). After washing with pure water, the cell suspension was stained for 1 h with uranyl actetate solution in the dark (1% in solution in ultrapure water prepared from depleted

uranyl acetate dihydrate purchased from EMS, Hatfield). Subsequently, the sample was again washed with pure water prior to dehydration by an ethanol/water series (50%, 70%, 90%, 2 × 100% dry EtOH, purified with a Solvent Purification System, stored over molecular sieves). The dehydrated samples were then transferred into BEEM capsules (Plano, Wetzlar). After removal of the ethanol, the cell suspension was immersed in mixtures of Embed 812 (EMS, Hatfield) and ethanol (Embed/EtOH = 1:1 v/v for 1 hour, 2:1 v/v for 12 h) and prior to embedding in pure Embed 812 for 4 h. After a further change of the embedding medium, the resin was allowed to harden in an oven at 70 °C for 24 h. From the resin block, ultrathin sections of 80 nm were cut with an ultramicrotome (PT-XL PowerTome, RMC, Tucson) using a diamond knife (RMC, Tucson). The ultrathin resin sections were captured, deposited on a carbon supported copper grid (400 mesh, Quantifoil, Jena) and imaged with a Technai G2 system (FEI), with 120 kV acceleration voltage in STEM mode (HAADF detection).

Statistical analysis

The result values represent the mean ± SD ($n \geq 3$). To determine the Pearson correlation, the PEARSON function in Excel was used. Each parameter was compared to the transfection efficiency at N/P 20. The t-test calculation was done using the t-test function in excel. The hemolysis data of the library at 10 $\mu g\ mL^{-1}$ was compared with the values of PMA.

ACKNOWLEDGEMENT

The authors like to thank the Bundesministerium für Bildung und Forschung (BMBF, Germany, #031A518B Vectura, #13N13416 smart-dye-livery, #13XP5034A PolyBioMik) for financial support. Furthermore, funding of the collaborative research center PolyTarget (SFB 1278) by the Deutsche Forschungsgemeinschaft (DFG) is highly acknowledged. A. Traeger acknowledges the Carl Zeiss Foundation for funding. M. Reifarth is grateful for financial support in the frames of "Carl-Zeiss-Strukturmaßnahme" as well as the ProExzellenzII initiative "Nanopolar" of the Federal State of Thuringia. J. C. Brendel thanks the Deutsche Forschungsgemeinschaft (DFG) for generous funding in the Emmy-Noether Programm (BR 4905/3-1). The authors furthermore acknowledge Elisabeth Preußger and Carolin Kellner for assistance with cell experiments. TEM investigations were performed at the electron microscopy facilities of the Jena Center for Soft Matter (JCSM), which was established with grants from the Deutsche Forschungsgemeinschaft (DFG) and the European Fund for Regional Development (EFRE). The LSM880 ELYRA PS.1 was further funded with a grant from the DFG.

SUPPORTING INFORMATION

Supporting NMR spectra, titration curves, buffer capacity plot, example for a Boltzmann fit for CC_{50} calculation, energy dependent uptake studies and example of the ImageJ analysis of the fluorescence microscopy pictures can be found in the supporting information.

CONFLICT OF INTEREST DISCLOSURE

The authors declare no competing financial interest.

ABBREVIATION

AEMA	(2-Aminoethyl)-methacrylate
MAEMA	*N*-Methyl-(2-aminoethyl)-methacrylate
DMAEMA	*N,N*-Dimethyl-(2-aminoethyl)-methacrylate
pDNA	Plasmid DNA
lPEI	Linear poly(ethylene imine)
bPEI	Branched poly(ethylene imine)
RAFT	Reversible addition-fragmentation chain transfer
Boc	*tert*-Butyloxycarbonyl
CTA	Chain transfer agent
I	Initiator
M	Monomer
PD	Poly(DMAEMA)
PM	Poly(MAEMA)
PA	Poly(AEMA)
PDM	Poly(DMAEMA-*co*-MAEMA)
PDA	Poly(DMAEMA-*co*-AEMA)
PMA	Poly(MAEMA-*co*-AEMA)
PDMA	Poly(DMAEMA-*co*-MAEMA-*co*-AEMA)
M_n	Number average molar mass
PMMA	Poly(methylmethacrylate)
DmAc	Dimethyl acetamid
HSQC	Heteronuclear single quantum coherence
AF4	Asymmetric flow field-flow fractionation
MALLS	Multi-angle laser light scattering
SEC	Size exclusion chromatography
TFA	Trifluoroacetic acid

CC_{50}	50% Cytotoxic concentration
S.D.	Standard deviation
TE	Transfection efficiency
EGFP	Enhanced green fluorescence protein
FCS	Fetal calf serum
HEK	Human embryonic kidney cells
MFI	Mean fluorescence intensity
HAADF-STEM	High-angle annular dark-field scanning transmission electron microscopy

REFERENCES

1 Lechardeur, D., Sohn, K.-J., Haardt, M., Hoshi, P. B., Monck, M., Graham, R. W., Beatty, B., Squire, J., O'Brodovich, H., and Lukacs, G. L. (1999) Metabolic instability of plasmid DNA in the cytosol: a potential barrier to gene transfer. *Gene Ther. 6*, 482-497.

2 Kealy, B., Liew, A., McMahon, J. M., Ritter, T., O'Doherty, A., Hoare, M., Greiser, U., Vaughan, E. E., Maenz, M., O'Shea, C., et al. (2009) Comparison of viral and nonviral vectors for gene transfer to human endothelial progenitor cells. *Tissue Eng. Part C-Me. 15*, 223-231.

3 Nayerossadat, N., Maedeh, T., and Ali, P. (2012) Viral and nonviral delivery systems for gene delivery. *Adv. Biomed. Res. 1*, 27-27.

4 Vaheri, A., and Pagano, J. S. (1965) Infectious poliovirus RNA: A sensitive method of assay. *Virology 27*, 434-6.

5 De Smedt, S. C., Demeester, J., and Hennink, W. E. (2000) Cationic polymer based gene delivery systems. *Pharm. Res. 17*, 113-126.

6 Wu, G. Y., and Wu, C. H. (1987) Receptor-mediated in vitro gene transformation by a soluble DNA carrier system. *J. Biol. Chem. 262*, 4429-32.

7 Wong, S. Y., Pelet, J. M., and Putnam, D. (2007) Polymer systems for gene delivery—Past, present, and future. *Prog. Polym. Sci. 32*, 799-837.

8 Boussif, O., Lezoualc'h, F., Zanta, M. A., Mergny, M. D., Scherman, D., Demeneix, B., and Behr, J. P. (1995) A versatile vector for gene and oligonucleotide transfer into cells in culture and in vivo: polyethylenimine. *Proc. Natl. Acad. Sci. U. S. A. 92*, 7297-301.

9 Behr, J. P. (1997) The proton sponge: A trick to enter cells the viruses did not exploit. *Chimia 51*, 34-36.

10 Ahmed, M., and Narain, R. (2013) Progress of RAFT based polymers in gene delivery. *Prog. Polym. Sci. 38*, 767-790.

11 Xu, F. J., Neoh, K. G., and Kang, E. T. (2009) Bioactive surfaces and biomaterials via atom transfer radical polymerization. *Prog. Polym. Sci. 34*, 719-761.

12 Zhu, C., Jung, S., Si, G., Cheng, R., Meng, F., Zhu, X., Park, T. G., and Zhong, Z. (2010) Cationic methacrylate copolymers containing primary and tertiary amino side groups: Controlled synthesis via RAFT polymerization, DNA condensation, and in vitro gene transfection. *J. Polym. Sci. A: Polym. Chem. 48*, 2869-2877.

13 Sprouse, D., and Reineke, T. M. (2014) Investigating the effects of block versus statistical glycopolycations containing primary and tertiary amines for plasmid DNA delivery. *Biomacromolecules 15*, 2616-2628.

14 Smith, A. E., Sizovs, A., Grandinetti, G., Xue, L., and Reineke, T. M. (2011) Diblock glycopolymers promote colloidal stability of polyplexes and effective pDNA and siRNA delivery under physiological salt and serum conditions. *Biomacromolecules 12*, 3015-3022.

15 Palermo, E. F., Lee, D.-K., Ramamoorthy, A., and Kuroda, K. (2011) Role of cationic group structure in membrane binding and disruption by amphiphilic copolymers. *J. Phys. Chem. B 115*, 366-375.

16 Funhoff, A. M., van Nostrum, C. F., Koning, G. A., Schuurmans-Nieuwenbroek, N. M. E., Crommelin, D. J. A., and Hennink, W. E. (2004) Endosomal escape of polymeric gene delivery complexes is not always enhanced by polymers buffering at low pH. *Biomacromolecules 5*, 32-39.

17 Nakase, I., Kobayashi, S., and Futaki, S. (2010) Endosome-disruptive peptides for improving cytosolic delivery of bioactive macromolecules. *Pept. Sci. 94*, 763-770.

18 Murthy, N., Robichaud, J. R., Tirrell, D. A., Stayton, P. S., and Hoffman, A. S. (1999) The design and synthesis of polymers for eukaryotic membrane disruption. *J. Control. Release 61*, 137-143.

19 Lowe, A. B., and McCormick, C. L. (2007) Reversible addition–fragmentation chain transfer (RAFT) radical polymerization and the synthesis of water-soluble (co)polymers under homogeneous conditions in organic and aqueous media. *Prog. Polym. Sci. 32*, 283-351.

20 Fixe, F., Dufva, M., Telleman, P., and Christensen, C. B. V. (2004) Functionalization of poly(methyl methacrylate) (PMMA) as a substrate for DNA microarrays. *Nucleic Acids Res. 32*, e9.

21 Moad, G., Chong, Y. K., Postma, A., Rizzardo, E., and Thang, S. H. (2005) Advances in RAFT polymerization: the synthesis of polymers with defined end-groups. *Polymer 46*, 8458-8468.

22 Thomas, D. B., Convertine, A. J., Hester, R. D., Lowe, A. B., and McCormick, C. L. (2004) Hydrolytic susceptibility of dithioester chain transfer agents and implications in aqueous RAFT polymerizations. *Macromolecules 37*, 1735-1741.

23 Xu, J., He, J., Fan, D., Wang, X., and Yang, Y. (2006) Aminolysis of polymers with thiocarbonylthio termini prepared by RAFT polymerization: The difference between polystyrene and polymethacrylates. *Macromolecules 39*, 8616-8624.

24 Sinclair, A., Bai, T., Carr, L. R., Ella-Menye, J.-R., Zhang, L., and Jiang, S. (2013) Engineering buffering and hydrolytic or photolabile charge shifting in a polycarboxybetaine ester gene delivery platform. *Biomacromolecules 14*, 1587-1593.

25 Kuroda, K., and DeGrado, W. F. (2005) Amphiphilic polymethacrylate derivatives as antimicrobial agents. *J. Am. Chem. Soc. 127*, 4128-4129.

26 Palermo, E. F., Vemparala, S., and Kuroda, K. (2012) Cationic spacer arm design strategy for control of antimicrobial activity and conformation of amphiphilic methacrylate random copolymers. *Biomacromolecules 13*, 1632-1641.

27 Li, H., Cortez, M. A., Phillips, H. R., Wu, Y., and Reineke, T. M. (2013) Poly(2-deoxy-2-methacrylamido glucopyranose)-b-Poly(methacrylate amine)s: Optimization of diblock glycopolycations for nucleic acid delivery. *ACS Macro Lett. 2*, 230-235.

28 Rinkenauer, A. C., Schubert, S., Traeger, A., and Schubert, U. S. (2015) The influence of polymer architecture on in vitro pDNA transfection. *J. Mater. Chem. B 3*, 7477-7493.

29 Layman, J. M., Ramirez, S. M., Green, M. D., and Long, T. E. (2009) Influence of polycation molecular weight on poly(2-dimethylaminoethyl methacrylate)-mediated DNA delivery in vitro. *Biomacromolecules 10*, 1244-1252.

30 Wagner, M., Pietsch, C., Tauhardt, L., Schallon, A., and Schubert, U. S. (2014) Characterization of cationic polymers by asymmetric flow field-flow fractionation and multi-angle light scattering—A comparison with traditional techniques. *J. Chromatogr. A 1325*, 195-203.

31 Perevyazko, I., Trützschler, A.-K., Gubarev, A., Lebedeva, E., Traeger, A., Schubert, U. S., and Tsvetkov, N. (2017) Molecular and structural analysis via hydrodynamic methods: Cationic poly(2-aminoethyl-methacrylate)s. *Polymer 131*, 252-262.

32 van de Wetering, P., Zuidam, N. J., van Steenbergen, M. J., van der Houwen, O. A. G. J., Underberg, W. J. M., and Hennink, W. E. (1998) A mechanistic study of the hydrolytic stability of poly(2-(dimethylamino)ethyl methacrylate). *Macromolecules 31*, 8063-8068.

33 Chiriac, V., and Balea, G. (1997) Buffer index and buffer capacity for a simple buffer solution. *J. Chem. Educ. 74*, 937.

34 Fischer, D., Li, Y., Ahlemeyer, B., Krieglstein, J., and Kissel, T. (2003) In vitro cytotoxicity testing of polycations: influence of polymer structure on cell viability and hemolysis. *Biomaterials 24*, 1121-1131.

35 Kleinberger, R. M., Burke, N. A. D., Zhou, C., and Stöver, H. D. H. (2016) Synthetic polycations with controlled charge density and molecular weight as building blocks for biomaterials. *J. Biomater. Sci., Polym. Ed. 27*, 351-369.

36 Lepecq, J. B., and Paoletti, C. (1967) A fluorescent complex between ethidium bromide and nucleic acids. *J. Mol. Biol. 27*, 87-106.

37 Geall, A. J., and Blagbrough, I. S. (2000) Rapid and sensitive ethidium bromide fluorescence quenching assay of polyamine conjugate–DNA interactions for the analysis of lipoplex formation in gene therapy. *J. Pharm. Biomed. Anal. 22*, 849-859.

38 Rinkenauer, A. C., Tauhardt, L., Wendler, F., Kempe, K., Gottschaldt, M., Traeger, A., and Schubert, U. S. (2015) A cationic poly(2-oxazoline) with high in vitro transfection efficiency identified by a library approach. *Macromol. Biosci. 15*, 414-425.

39 You, Y.-Z., Manickam, D. S., Zhou, Q.-H., and Oupický, D. (2007) Reducible poly(2-dimethylaminoethyl methacrylate): Synthesis, cytotoxicity, and gene delivery activity. *J. Control. Release 122*, 217-225.

40 Agarwal, S., Zhang, Y., Maji, S., and Greiner, A. (2012) PDMAEMA based gene delivery materials. *Mater. Today 15*, 388-393.

41 van de Wetering, P., Moret, E. E., Schuurmans-Nieuwenbroek, N. M. E., van Steenbergen, M. J., and Hennink, W. E. (1999) Structure−activity relationships of water-soluble cationic methacrylate/methacrylamide polymers for nonviral gene delivery. *Bioconjugate Chem. 10*, 589-597.

42 Pezzoli, D., Giupponi, E., Mantovani, D., and Candiani, G. (2017) Size matters for in vitro gene delivery: investigating the relationships among complexation protocol, transfection medium, size and sedimentation. *Sci. Rep. 7*, 44134.

43 Kwok, A., and Hart, S. L. Comparative structural and functional studies of nanoparticle formulations for DNA and siRNA delivery. *Nanomedicine: Nanotechnology, Biology and Medicine 7*, 210-219.

44 Jain, R., Dandekar, P., Loretz, B., Koch, M., and Lehr, C.-M. (2015) Dimethylaminoethyl methacrylate copolymer-siRNA nanoparticles for silencing a therapeutically relevant gene in macrophages. *MedChemComm 6*, 691-701.

45 Xu, F. J., and Yang, W. T. (2011) Polymer vectors via controlled/living radical polymerization for gene delivery. *Prog. Polym. Sci. 36*, 1099-1131.

46 Schallon, A., Jérôme, V., Walther, A., Synatschke, C. V., Müller, A. H. E., and Freitag, R. (2010) Performance of three PDMAEMA-based polycation architectures as gene delivery agents in comparison to linear and branched PEI. *React. Funct. Polym. 70*, 1-10.

47 Cherng, J.-Y., van de Wetering, P., Talsma, H., Crommelin, D. J. A., and Hennink, W. E. (1996) Effect of size and serum proteins on transfection efficiency of poly ((2-dimethylamino)ethyl methacrylate)-plasmid nanoparticles. *Pharm. Res. 13*, 1038-1042.

48 Ogris, M., Brunner, S., Schuller, S., Kircheis, R., and Wagner, E. (1999) PEGylated DNA/transferrin-PEI complexes: reduced interaction with blood components, extended circulation in blood and potential for systemic gene delivery. *Gene Ther. 6*, 595-605.

49 Monopoli, M. P., Walczyk, D., Campbell, A., Elia, G., Lynch, I., Baldelli Bombelli, F., and Dawson, K. A. (2011) Physical−chemical aspects of protein corona: Relevance to in vitro and in vivo biological impacts of nanoparticles. *J. Am. Chem. Soc. 133*, 2525-2534.

50 Ogris, M., Brunner, S., Schüller, S., Kircheis, R., and Wagner, E. (1999) PEGylated DNA/transferrin–PEI complexes: reduced interaction with blood components, extended circulation in blood and potential for systemic gene delivery. *Gene Ther. 6*, 595.

51 Forrest, M. L., Meister, G. E., Koerber, J. T., and Pack, D. W. (2004) Partial acetylation of polyethylenimine enhances in vitro gene delivery. *Pharm. Res. 21*, 365-371.

52 van de Wetering, P., Cherng, J.-Y., Talsma, H., and Hennink, W. E. (1997) Relation between transfection efficiency and cytotoxicity of poly(2-(dimethylamino)ethyl methacrylate)/plasmid complexes. *J. Control. Release 49*, 59-69.

53 Dubruel, P., Christiaens, B., Vanloo, B., Bracke, K., Rosseneu, M., Vandekerckhove, J., and Schacht, E. (2003) Physicochemical and biological evaluation of cationic polymethacrylates as vectors for gene delivery. *Eur. J. Pharm. Sci. 18*, 211-220.

54 Jones, R. A., Poniris, M. H., and Wilson, M. R. (2004) pDMAEMA is internalised by endocytosis but does not physically disrupt endosomes. *J. Control. Release 96*, 379-391.

55 Forrest, M. L., and Pack, D. W. (2002) On the kinetics of polyplex endocytic trafficking: implications for gene delivery vector design. *Mol. Ther. 6*, 57-66.

56 Kulkarni, R. P., Mishra, S., Fraser, S. E., and Davis, M. E. (2005) Single cell kinetics of intracellular, nonviral, nucleic acid delivery vehicle acidification and trafficking. *Bioconjugate Chem. 16*, 986-994.

57 Vercauteren, D., Rejman, J., Martens, T. F., Demeester, J., De Smedt, S. C., and Braeckmans, K. (2012) On the cellular processing of non-viral nanomedicines for nucleic acid delivery: Mechanisms and methods. *J. Control. Release 161*, 566-581.

58 Rejman, J., Bragonzi, A., and Conese, M. (2005) Role of clathrin- and caveolae-mediated endocytosis in gene transfer mediated by lipo- and polyplexes. *Mol. Ther. 12*, 468-474.

59 Bieber, T., Meissner, W., Kostin, S., Niemann, A., and Elsasser, H.-P. (2002) Intracellular route and transcriptional competence of polyethylenimine–DNA complexes. *J. Control. Release 82*, 441-454.

60 Rehman, Z. U., Hoekstra, D., and Zuhorn, I. S. (2013) Mechanism of polyplex- and lipoplex-mediated delivery of nucleic acids: Real-time visualization of transient membrane destabilization without endosomal lysis. *ACS Nano 7*, 3767-3777.

61 Bonner, D. K., Leung, C., Chen-Liang, J., Chingozha, L., Langer, R., and Hammond, P. T. (2011) Intracellular trafficking of polyamidoamine–poly(ethylene glycol) block copolymers in DNA delivery. *Bioconjugate Chem. 22*, 1519-1525.

62 Salomone, F., Cardarelli, F., Di Luca, M., Boccardi, C., Nifosì, R., Bardi, G., Di Bari, L., Serresi, M., and Beltram, F. (2012) A novel chimeric cell-penetrating peptide with membrane-disruptive properties for efficient endosomal escape. *J. Control. Release 163*, 293-303.

63 Reifarth, M., Hoeppener, S., and Schubert, U. S. (2018) Uptake and intracellular fate of engineered nanoparticles in mammalian cells: Capabilities and limitations of transmission electron microscopy—polymer-based nanoparticles. *Adv. Mater. 30*, 1703704.

64 Bus, T., Englert, C., Reifarth, M., Borchers, P., Hartlieb, M., Vollrath, A., Hoeppener, S., Traeger, A., and Schubert, U. S. (2017) 3rd generation poly(ethylene imine)s for gene delivery. *J. Mater. Chem. B 5*, 1258-1274.

65 Palermo, E. F., Sovadinova, I., and Kuroda, K. (2009) Structural determinants of antimicrobial activity and biocompatibility in membrane-disrupting methacrylamide random copolymers. *Biomacromolecules 10*, 3098-3107.

66 Vaidyanathan, S., Chen, J., Orr, B. G., and Banaszak Holl, M. M. (2016) Cationic polymer intercalation into the lipid membrane enables intact polyplex DNA escape from endosomes for gene delivery. *Mol. Pharm. 13*, 1967-1978.

67 Vaidyanathan, S., Anderson, K. B., Merzel, R. L., Jacobovitz, B., Kaushik, M. P., Kelly, C. N., van Dongen, M. A., Dougherty, C. A., Orr, B. G., and Banaszak Holl, M. M. (2015) Quantitative measurement of cationic polymer vector and polymer-pDNA polyplex intercalation into the cell plasma membrane. *ACS Nano 9*, 6097-109.

TOC

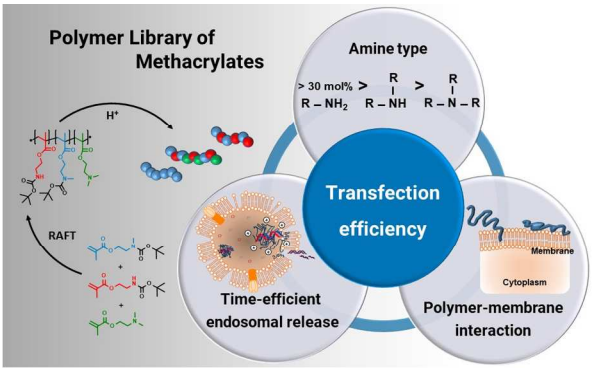
Polymer Library of Methacrylates
H+
RAFT
Amine type
> 30 mol%
R – NH2
R – NH
R – N – R
Transfection efficiency
Time-efficient endosomal release
Membrane
Cytoplasm
Polymer-membrane interaction